



Multivariate Likelihood Search for Single-Top-Quark Production with 1 fb^{-1}

The CDF Collaboration
URL <http://www-cdf.fnal.gov>
(Dated: November 4, 2006)

We report results from a search for single-top-quark production in a 0.955 fb^{-1} dataset accumulated with the CDF II detector. We employ a multivariate likelihood method to analyze the data. No significant evidence of a signal is found, and 95% confidence level limits are set under various scenarios.

Preliminary Results for Winter 2007 Conferences

I. INTRODUCTION

According to the Standard Model, in $p\bar{p}$ collisions at the Tevatron top quarks can be created in pairs via the strong force, or singly via the electroweak interaction. The latter production mode is referred to as “single-top-quark” production and takes place mainly through the s - or t -channel exchange of a W boson (Figure 1). The CDF and DØ collaborations have published single-top results at $\sqrt{s} = 1.8$ TeV and $\sqrt{s} = 1.96$ TeV [1, 2]. None of these studies established single-top evidence, and 95% confidence level (C.L.) upper limits on the single-top production cross section were set.

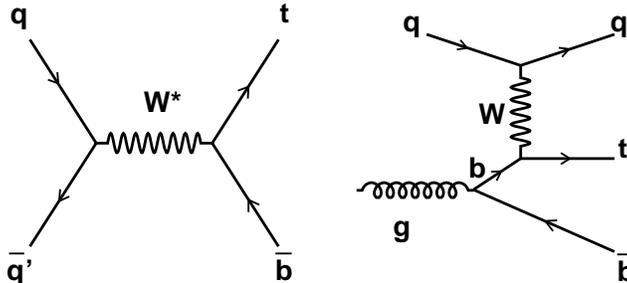


FIG. 1: Representative Feynman diagrams for single-top-quark production at the Tevatron: s-channel W^* (left) and t-channel W -gluon fusion (right).

Studying single-top production at hadron colliders is important for a number of reasons. First, it provides the only window into measuring the CKM matrix element $|V_{tb}|^2$, which in turn is closely tied to the number of quark generations. Second, measuring the spin polarization of single-top quarks can be used to test the V-A structure of the top weak charged current interaction. Third, single-top events represent an irreducible background to several searches for SM or non-SM signals, as for example Higgs boson searches. Fourth and last, the presence of various new SM and non-SM phenomena may be inferred by observing deviations from the predicted rate of the single-top signal.

The theoretical single-top production cross section is $\sigma_{s+t} = 2.9$ pb for a top mass of 175 GeV/ c^2 [3]. Despite this small rate, the main obstacle in finding single-top is in fact the large associated background. After all selection requirements are imposed, the signal to background ratio is close to 1/10. This challenging, background-dominated dataset is the main motivation for using multivariate techniques. The following sections present the event selection, the signal and background estimations, an extended b -tagger and a kinematic fitter used to improve signal identification, the statistical techniques and the expected and observed single-top cross section results, and a brief summary of these results.

II. SELECTION REQUIREMENTS

A. Trigger

Events for this analysis are selected with a high- E_T electron trigger or a high- P_T muon trigger, both at 18 GeV and measured in the central subdetectors ($|\eta| < 1$). An addition to the analysis was the inclusion of a forward electron trigger which selects events with one high- E_T electron (20 GeV) and $1 < |\eta| < 2$, and large missing transverse energy \cancel{E}_T (15 GeV). While the plug calorimeters extend beyond $|\eta| > 3$, the pseudorapidity range is restricted due to the additional requirement that the calorimeter energy cluster matches to a track measured in the silicon detector, which only covers the $|\eta| < 2$ region.

B. Event Selection

Our selection exploits the kinematic features of the signal final state, which contains a top quark, a bottom quark, and possibly additional light quark jets. To reduce multijet backgrounds, the W originating from the top quark is required to have decayed leptonically. We demand therefore a high-energy electron or muon ($E_T(e) > 20$ GeV, or $P_T(\mu) > 20$ GeV/ c) and large missing energy from the undetected neutrino $\cancel{E}_T > 25$ GeV. We reject dilepton events from $t\bar{t}$ and Z decays by requiring the dilepton mass to be outside the range: 76 GeV/ $c^2 < M_{\ell\ell} < 106$ GeV/ c^2 . The

Process	2 jets
t -channel	22.36 ± 3.64
s -channel	15.44 ± 2.23
$t\bar{t}$	58.35 ± 13.46
WW	5.51 ± 0.94
WZ	7.96 ± 0.79
ZZ	0.25 ± 0.06
$Z \rightarrow \tau\tau$	5.49 ± 2.41
$Z \rightarrow \mu\mu$	5.25 ± 1.54
$Z \rightarrow ee$	1.18 ± 0.45
Total MC-based background	121.79 ± 13.10

TABLE I: Number of $W + 2$ jets events expected from signal, $t\bar{t}$, diboson, and $Z \rightarrow \ell\ell(+\text{jets})$ in the 0.955 fb^{-1} dataset.

Process	2 jets
Non- W	26.2 ± 15.9
Mistags	136.1 ± 19.7
$Wb\bar{b}$	170.7 ± 50.7
$Wc\bar{c}$	63.5 ± 19.9
Wc	68.6 ± 19.0
Total data-based (all above)	465.3 ± 93.1
Single-top	37.8 ± 2.8
Total MC-based (no single-top)	84.0 ± 19.7
Total Expected	587.1 ± 96.6
Observed	644

TABLE II: Expected and observed numbers of $W + 2$ jets events after all selection requirements have been imposed.

backgrounds surviving these selections can be classified as “non-top” and $t\bar{t}$. The non-top backgrounds are: $Wb\bar{b}$, $Wc\bar{c}$, Wc , mistags (light quarks misidentified as heavy flavor jets), non- W (events where a jet is erroneously identified as a lepton), and diboson WW , WZ , and ZZ . We remove a large fraction of the non-top and $t\bar{t}$ backgrounds by demanding exactly two jets with $E_T > 15 \text{ GeV}$ and $|\eta| < 2.8$ be present in the event. At least one of these two jets should be tagged as a b -quark jet by using displaced vertex information from the silicon vertex detector (SVX). In events with an identified electron, the non- W content is substantially reduced by making certain requirements on the angle between the \cancel{E}_T vector and the transverse momentum vectors of the leading and second leading jets: $\Delta\Phi(\cancel{E}_T - J_1)$ and $\Delta\Phi(\cancel{E}_T - J_2)$ [4].

III. SIGNAL AND BACKGROUND ESTIMATIONS

Depending on the method by which their contributions are estimated, the different processes can be classified into two categories: Monte Carlo-based or data-based estimations. For example, the $t\bar{t}$, diboson (WW , WZ and ZZ) contributions, and $Z \rightarrow \ell\ell$ belong to the first category. The same can be said about signal estimations. For all these processes, the contributions are estimated using a combination of Monte Carlo-generated samples (to extract acceptance and efficiency factors) and the theoretical cross sections (to normalize the rates).[5] Table I shows the expected yields in the 0.955 fb^{-1} dataset.

The other category contains those background processes whose estimations require the use of CDF data: W +heavy flavor ($Wb\bar{b}$, $Wc\bar{c}$, Wc), mistags, and non- W events. Their contributions are obtained using a similar method with that employed in Ref.[6], with two differences. One difference is the larger η range for the jet definition ($|\eta| < 2.8$) used in this search. The other differences are the inclusion of the forward electron events and a different estimation of the non- W background component by fitting the \cancel{E}_T spectrum. The expected and observed event yields corresponding to the 0.955 fb^{-1} dataset are given in Table II.

IV. SPECIAL EVENT VARIABLES

A. ANN extended B -tagger

An Artificial Neural Network (ANN) [7] was developed to increase the b -quark purity of the sample selected by the standard b -tagging algorithm. The latter is based on measuring displaced (secondary) vertices, and in addition to b -jets it also selects a significant fraction of c - and light flavor jets as well (as much as 50%). The extended (ANN) tagger is applied to jets selected by the standard b -tagger, and exploits mainly the long lifetime (1.6 ps) of b -hadrons. Other features used by the ANN are the high b -quark mass, the high decay multiplicity, and the decay into leptons. For illustration, Fig. 2 shows good shape agreement between the ANN output distributions for the $W + 2$ jet data and a sum of the individual background components normalized to data.

As a measure of the power provided by this tool, we note that using the ANN output to select events in the single-top analysis would lead to a reduction of more than 60% of non- b vertices while keeping about 82% of real b vertices. In the analysis however we will not cut on the ANN tagger output, but rather use this output as an event variable.

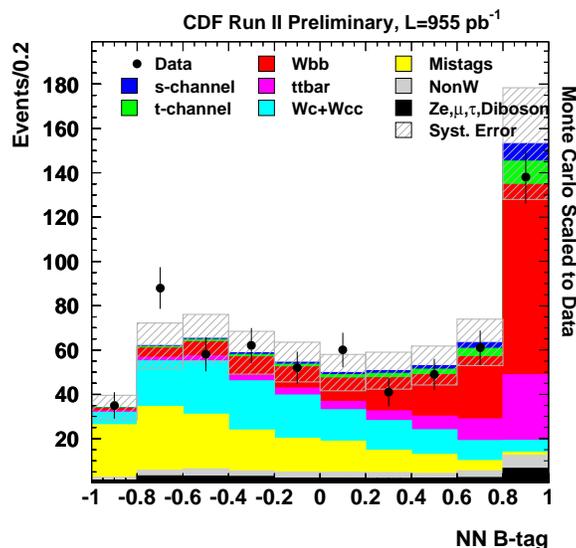


FIG. 2: The ANN tagger output distributions for the CDF $W+2$ jets events (points) compared to the Monte Carlo expectations.

B. Kinematic Fitter

Some of the variables used in our analysis require knowledge of the top rest frame. Other variables, such as the MADGRAPH matrix element are very sensitive to $M_{\ell\nu b}$, which is poorly measured compared to the width of the pole in the propagator in the matrix element. If we use the measured four-vectors for the two jets, the missing transverse energy and the lepton directly in the matrix element, we will get a random contribution from the mismeasured top mass which is mistakenly interpreted to be far off-shell. One of the main purposes of the kinematic fit is to find the four-vectors of the b -decay jet and the neutrino which are the most consistent with the measured values and which have the top quark on shell. A similar problem arises with the measured mass of the lepton and neutrino four-vectors. If these depart from the W mass, the matrix element can be very small due to the W propagator. The mass of the $\ell\nu$ system is forced to m_W , but this fails in about 30% of events because of the values of the lepton momentum and missing transverse energy vectors do not allow a real solution of P_z for the neutrino. The kinematic fit χ^2 function includes a term which steers the fit to find real solutions for the neutrino momentum.

There are five quantities which are quite imprecisely measured: $(P_x(b), P_y(b), P_z(b))$ and $(P_x(\nu), P_y(\nu))$. These variables can be bijectively mapped to (P_b, η_b, Φ_b) and $(\cancel{E}_T, \cancel{\Phi}_\nu)$. Assuming that the b quark direction is reasonably well measured, then there are only three quantities we will allow to float in the kinematic fit: $(P_b, \cancel{E}_T, \cancel{\Phi}_\nu)$.

The following ideas form the basis for the kinematic fitter:

1. Allow P_b , \cancel{E}_T , \cancel{P}_ν to float within their uncertainties around their measured values.
2. Constrain the mass of the lepton- ν pair to $M_W = 80.4 \text{ GeV}/c^2$, and derive the two neutrino solutions P_{z1} and P_{z2} (analytical functions of \cancel{E}_T and \cancel{P}_ν).
3. Construct a χ^2 function:

$$\chi^2 = \frac{(P_b - P_b^{obs})^2}{\sigma_{P_b}^2} + \frac{(\cancel{E}_T - \cancel{E}_T^{obs})^2}{\sigma_{\cancel{E}_T}^2} + \frac{(\cancel{P}_\nu - \cancel{P}_\nu^{obs})^2}{\sigma_{\cancel{P}_\nu}^2} + \frac{(M_{\ell\nu b} - M_t)^2}{\sigma_{M_t}^2} + Y(\text{Im}(P_z))^2$$

4. We minimize the χ^2 above with respect to P_b , \cancel{E}_T , \cancel{P}_ν , under four scenarios:
 - a. χ_1^2 , χ_3^2 in which we assume jet j_1 comes from top decay and use the two neutrino solutions P_{z1} and P_{z2} in calculating $M_{\ell\nu b}$.
 - b. χ_2^2 , χ_4^2 in which we assume jet j_2 comes from top decay and use the two neutrino solutions P_{z1} and P_{z2} in calculating $M_{\ell\nu b}$.

The χ^2 values above will be used to select the b -jet from top decay, to select the P_z solution for the neutrino, or simply as event variables.

V. LIKELIHOOD FUNCTION TECHNIQUE

No single variable encodes all conceivable signal-background separation, and so a likelihood function [8] is proposed to combine several variables together into a discriminant which can be used to compute limits or to discover a signal.

The likelihood function \mathcal{L} is constructed by first forming histograms of each variable (n_i bins per variable), separately for the signal distributions and for several background distributions, denoted f_{ijk} for bin j of variable i for the event class k . For the signal, $k = 1$, and in this note, four background classes are considered: $Wb\bar{b}$, $t\bar{t}$, $Wc\bar{c}/Wc$, and mistags, which are event classes 2, 3, 4 and 5. These histograms are normalized such that $\sum_{j=1}^{n_i} f_{ijk} = 1$ for all i and all k . The likelihood function for an event is computed by evaluating in which bin j_i in which the event falls in the distribution of variable i , and computing

$$p_{ik} = \frac{f_{ij_i k}}{\sum_{m=1}^5 f_{ij_i m}}, \quad (1)$$

which is used to compute

$$\mathcal{L}_k(\{x_i\}) = \frac{\prod_{i=1}^{n_{var}} p_{ik}}{\sum_{m=1}^5 \prod_{i=1}^{n_{var}} p_{im}}. \quad (2)$$

The signal likelihood function is the one which corresponds to the signal class of events, \mathcal{L}_1 .

Two likelihood functions are computed – one using the t -channel single-top signal in the signal reference histograms \mathcal{L}_t , and one using the s -channel single-top signal in the signal reference histograms \mathcal{L}_s .

A. t -channel Likelihood Function.

The t -channel likelihood function \mathcal{L}_t uses seven variables, and assumes the b -tagged jet comes from top decay:

1. H_T , the scalar sum of the E_T 's of the two jets, lepton E_T , and \cancel{E}_T .
2. $Q \times \eta$, the charge of the lepton times the pseudorapidity of the jet which is not b -tagged.
3. $M_{\ell\nu b}^{hyb}$, a hybrid reconstructed top mass formed using the raw reconstructed value of P_b , while taking the $P_z(\nu)$ from the kinematic fit (the solution corresponding to the lower of the two χ^2 values).
4. $\cos \theta_{t\text{-chan}}$, the cosine of the angle between the lepton and the untagged jet in the top decay frame.
5. M_{jj} , the invariant mass of the two jets.

6. $ME_{t\text{-chan}}$, the MADGRAPH matrix element computed using the constrained four-vectors of the b , ℓ and ν .
7. ANN b -tag output.

We show the \mathcal{L}_t likelihood function resulting from combining the above seven variables in Fig. 3. A good signal-background separation is apparent.

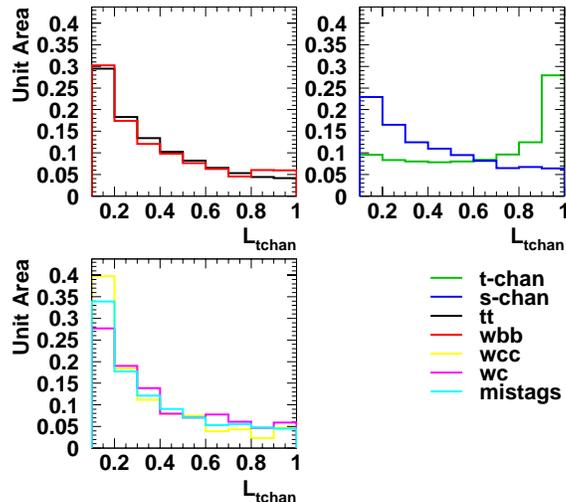


FIG. 3: The distributions of the t -channel likelihood function \mathcal{L}_t normalized to unit area.

B. s -channel Likelihood Function.

The s -channel likelihood function \mathcal{L}_s uses six variables and it is constructed in the same way as the t -channel likelihood. In fact, three of the variables are common to \mathcal{L}_t (numbers 1, 6, and 7 from the list given in the previous subsection). The other three variables are:

1. $M_{\ell\nu b}^{hyb2}$, a hybrid reconstructed top mass formed using the raw reconstructed value of P_b , while taking the $P_z(\nu)$ from the kinematic fit, and choosing the b -jet from top using a simple ANN function based on the difference of kinematic fitter χ^2 and the difference between the pseudorapidities of the jets.
2. $\log(M_{\ell\nu b}^{hyb2} \times H_T)$, the product of the s -channel optimized $M_{\ell\nu b}$ and H_T .
3. $E_T(j1)$, the transverse energy of the leading jet.

The \mathcal{L}_s likelihood function distributions are shown in Fig. 4. The \mathcal{L}_s distributions for signal reflect the fact that none of the above six variables separates s - from t - channel components well.

C. Statistical Method. Results.

In the previous two subsections we showed how multiple variables are combined to form the two likelihood functions \mathcal{L}_t and \mathcal{L}_s . Now we will describe how these two variables can be used to make statements about the single-top content of the CDF data. Our statistical approach follows the one presented in Ref. [9]. The CDF data is compared against two models at a time. One is the null hypothesis (H_0) which asserts that the Standard Model processes *without* single-top describes the data, while the other, referred to as the test hypothesis (H_1), asserts that the data are modeled by the SM processes *including* Standard Model single top. Our test statistic is:

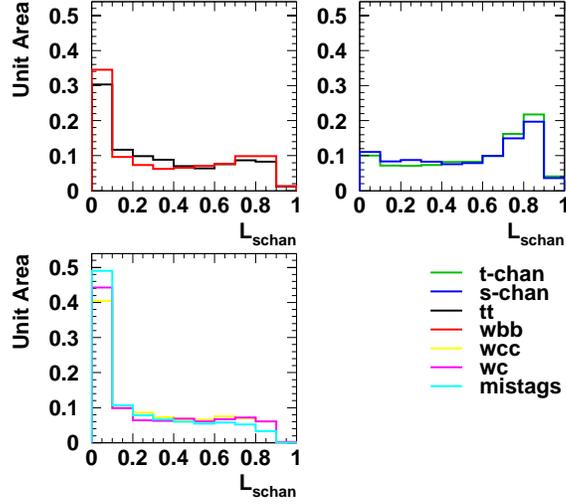


FIG. 4: The distributions of the s -channel likelihood function \mathcal{L}_s normalized to unit area. There is almost no separation between the s - and t - channel single-top distributions (upper right plot).

$$Q(\vec{d}) = -2 \cdot \ln \frac{P(\vec{d}|H1)}{P(\vec{d}|H0)}$$

where N_{bin} denotes the total number of bins in the likelihood function, $\vec{d} = (d_1, d_2, \dots, d_{N_{bin}})$ is the observed data distribution.

A large number of simulated experiments \vec{d} are drawn either from the $H1$ or the $H0$ hypotheses, and the corresponding $Q(\vec{d})$ values are stored in two separate histograms $f^{H1}(Q)$ and $f^{H0}(Q)$, respectively. The systematic uncertainties are accounted for as described in Ref. [9]. Both the rate and shape uncertainties are taken into account by choosing nuisance parameters randomly on each pseudoexperiment. The shape uncertainties are estimated from the shifted \mathcal{L}_t and \mathcal{L}_s histograms corresponding to MC samples in which the particular sources for systematic uncertainties are varied. This is simultaneously included along with the rate uncertainties which, for signal contribution, are listed in Table IV.

If for a given pseudoexperiment (or CDF data) we measure a value Q_{obs} , then the $f^{H1}(Q)$ and $f^{H0}(Q)$ distributions can be integrated in the region $Q > Q_{obs}$, and the following quantities can be defined:

$$CL_{s+b}(Q_{obs}) = \text{Prob}(Q \geq Q_{obs}|H1) = \int_{Q_{obs}}^{\infty} f^{H1}(Q) \cdot dQ \quad (3)$$

$$CL_b(Q_{obs}) = \text{Prob}(Q \geq Q_{obs}|H0) = \int_{Q_{obs}}^{\infty} f^{H0}(Q) \cdot dQ \quad (4)$$

$$CL_s(Q_{obs}) = \frac{CL_{s+b}}{CL_b} \quad (5)$$

CL_s will be used to define the 95% C.L. exclusion limits, and $1-CL_b$ is in statistics language a p -value, i.e. the probability that the $H0$ model fluctuated up to more than the pseudo-experiment data.

To perform the single-top measurement we use the two-dimensional distributions of \mathcal{L}_t vs. \mathcal{L}_s to measure the s + t signal combined rate and use a χ^2 fit to this distributions to extract the separate s - and t - channel distributions.

Results. In Fig. 5 we present the \mathcal{L}_t and \mathcal{L}_s distributions of the data events compared to the Monte Carlo prediction (contributions from Table II scaled to match data normalization). The combined search results are shown in the second

Expected CL_s	0.049
Observed CL_s	0.035
Expected $1 - CL_b$	0.025
Observed $1 - CL_b$	0.585
Expected limit σ_{95} (pb)	2.86
Observed limit σ_{95} (pb)	2.65

TABLE III: Observed and expected results for the combined $s + t$ search.

column of Table III. These results assume no signal (backgrounds only) in the null hypothesis $H0$. The test hypothesis $H1$ assumes backgrounds plus SM $s + t$ channel signal. The interpretation of the $s + t$ results in Table III is as follows:

1. The median CL_s in $H0$ pseudo-experiments is 4.9% indicating that a priori we have the sensitivity required (5%) to exclude the $H1$ hypothesis at 95% C.L. The observed CL_s is 3.5%, implying we barely exclude the test hypothesis. This result is not yet surprising, since 95% exclusion of a true hypothesis is expected to happen in 5% of possible outcomes.
2. The median $1 - CL_b$ in $H1$ pseudo-experiments is 2.5%, indicating that a priori 50% of the $H1$ pseudoexperiments give this p -value or less (approx. 2σ excess). The a posteriori result $1 - CL_b = 58.5\%$ shows good consistency between the data and the $H0$ hypothesis.
3. The expected 95% C.L. limit $\sigma_{95} = 2.9$ pb is obtained from testing different $H1$ hypotheses by modifying the signal rate from its SM value, until the expected CL_s becomes 5%. The observed 95% C.L. limit of $\sigma_{95} = 2.7$ pb is slightly higher than expected, mostly due to the slight excess seen in the signal region of the \mathcal{L}_s distribution.

We also compute the $\chi^2(data|H1)$. For each computation of χ^2 the nuisance parameters are allowed to float, and we minimize this χ^2 for all choices of cross sections σ_s and σ_t . The best-fit point is at $\sigma_s^{fit} = 0.1$ pb and $\sigma_t^{fit} = 0.2$ pb. The predictions [11] of σ_s and σ_t of additional models including top-flavor, FCNC Ztc , a fourth generation model, and a top-pion model are shown in Fig. 6 along with the SM prediction and the exclusion contours.

Syst. Source	t -channel	s -channel
ISR	$\pm 1\%$	$\pm 2\%$
FSR	$\pm 5\%$	$\pm 1\%$
Jet Energy	$\pm 1.8\%$	$\pm 1.2\%$
PDF	$\pm 2.5\%$	$\pm 2.2\%$
NN b tagger	$\pm 1\%$	$\pm 1\%$
Evt. detection eff	$\pm 8\%$	$\pm 8\%$
Luminosity	$\pm 6\%$	$\pm 6\%$

TABLE IV: Estimate of the fractional (relative) rate uncertainties on the $W + 2$ jets signal contribution.

VI. CONCLUSION

We analyzed the 0.955 fb^{-1} dataset in search of single-top-quark signal, using a multivariate likelihood technique. We find no evidence of a signal. The 95% C.L. observed limit on the $s + t$ combined single-top cross section using the 2D $(\mathcal{L}_s, \mathcal{L}_t)$ likelihood functions is 2.7 pb (expected limit 2.9 pb; no-signal null hypothesis is used). Using a χ^2 fit of the $(\mathcal{L}_s, \mathcal{L}_t)$ distribution we obtain the best fit values of $0.2_{-0.2}^{+0.9}$ pb and $0.1_{-0.1}^{+0.7}$ pb for the t -channel and s -channel, respectively.

Acknowledgments

We thank the Fermilab staff and the technical staffs of the participating institutions for their vital contributions. This work was supported by the U.S. Department of Energy and National Science Foundation; the Italian Istituto Nazionale di Fisica Nucleare; the Ministry of Education, Culture, Sports, Science and Technology of Japan; the Natural Sciences and Engineering Research Council of Canada; the National Science Council of the Republic of

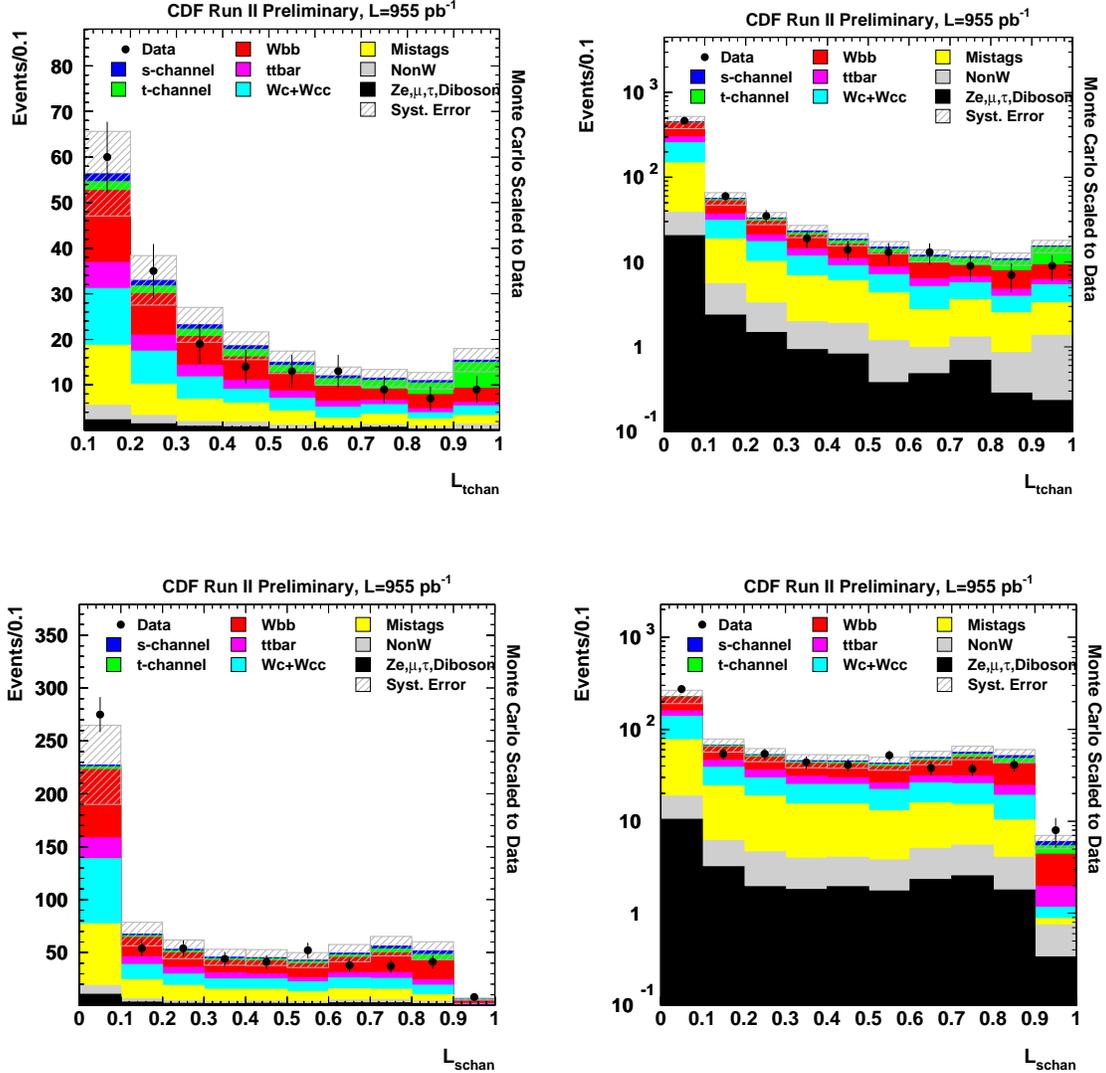


FIG. 5: The distributions of the t -channel (upper) and s -channel (lower) likelihood functions for CDF data compared to the Monte Carlo distributions normalized to the expected contributions. The Monte Carlo contributions are multiplied by 1.1 to match the data normalization. A linear (logarithmic) scale is used for the left (right) plots.

China; the Swiss National Science Foundation; the A.P. Sloan Foundation; the Bundesministerium fuer Bildung und Forschung, Germany; the Korean Science and Engineering Foundation and the Korean Research Foundation; the Particle Physics and Astronomy Research Council and the Royal Society, UK; the Russian Foundation for Basic Research; the Comision Interministerial de Ciencia y Tecnologia, Spain; and in part by the European Community's Human Potential Programme under contract HPRN-CT-20002, Probe for New Physics.

-
- [1] D. Acosta *et al.* (CDF Collaboration), Phys. Rev. D **65**, 091102 (2002); D. Acosta *et al.* (CDF Collaboration), Phys. Rev. D **69**, 052003 (2004); D. Acosta *et al.* (CDF Collaboration), Phys. Rev. D **71**, 012005 (2005).
 [2] B. Abbott *et al.* (DØ Collaboration), Phys. Rev. D **63**, 031101 (2001); V. M. Abazov *et al.* (DØ Collaboration), Phys. Lett. B **517**, 282 (2001); V. M. Abazov *et al.* (DØ Collaboration), Phys. Lett. B **622**, 265 (2005).
 [3] B. W. Harris *et al.*, Phys. Rev. D **66**, 054024 (2002); Z. Sullivan, Phys. Rev. D **70**, 114012 (2004).

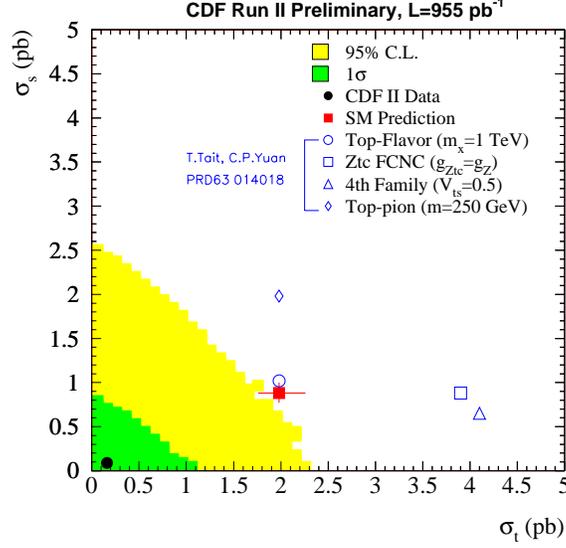


FIG. 6: The best fit value for σ_s and σ_t obtained from fitting the 2-dimensional \mathcal{L}_s vs. \mathcal{L}_t distribution. A $\Delta\chi^2$ is computed, comparing the $\chi^2(\sigma_s, \sigma_t)$ against that of best-fit corresponding to $(\sigma_s, \sigma_t) = (0.1 \text{ pb}, 0.2 \text{ pb})$. The 1σ fit region and the region allowed at the 95% C.L. are shown, along with the Standard Model prediction.

- [4] These requirements are: $\Delta\Phi(\cancel{E}_T - J_i) > A - \cancel{E}_T[\text{GeV}]/B$, with $A=\{1.9, 1.8\}$ and $B=\{20, 25\}$, for $i=\{1, 2\}$ if $|\eta_e| < 1.0$; and $A=\{0.3, 2.5\}$ and $B=\{\infty, 20\}$, for $i=\{1, 2\}$ if $|\eta_e| > 1.0$.
See S. Budd *et al.*, “Estimation and Modeling of Non-W Background for Single-Top Searches” CDF note no. 8489, 2006 (*internal*) and P.Dong *et al.*, “Reduction of QCD background in Lepton+Jets Events”, CDF note no. 8295, 2006 (*internal*)
- [5] S. Budd *et al.*, “Event detection efficiency for single-top events and MC based background estimate for Summer 2006”, CDF Note 8286, 2006 (*internal*). “Data based background estimate for Summer 2006 single-top search”, CDF note no. 8292. (*internal*)
- [6] The CDF Collaboration, “Measurement of the $t\bar{t}$ Production Cross Section in Vertex-Tagged Lepton+Jets Events” CDF Note 8810, 2006 (*public*)
- [7] M. Feindt, S. Richter, and W. Wagner, “A Neural Network b Tagger for Single-Top Analyses”, CDF note 7816, 2006 (*internal*).
- [8] R. Barlow, “Statistics: a Guide to the Use of Statistics in the Physical Sciences” John Wiley and Sons, LTD, West Sussex, England (1989).
- [9] T. Junk, “Sensitivity, Exclusion and Discovery with Small Signals, Large Backgrounds, and Large Systematics”, CDF note 8128 (*internal*). Also see: A. L. Read, J. Phys. G: Nucl. Part. Phys. **28**, 2693 (2002); P. Bock *et al.* (the LEP Collaborations), CERN-EP-98-046 (1998) and CERN-EP-2000-055 (2000).
- [10] M. Feindt, e-Print Archive physics/0402093 (2004).
- [11] T. Tait and C. P. Yuan, Phys.Rev. **D63** (2001) 014018, available online as arXiv:hep-ph/0007298 (2000).